Journal of Structural Geology, Vol. 16, No. 1, pp. 121 to 130, 1994
Printed in Great Britain

0191-8141/94 $06.00+0.00

Vorticity determination, distribution, partitioning and the heterogeneity and non-steadiness of natural deformations

DAZHI JIANG

Department of Geology, University of New Brunswick, P.O. Box 4400, Fredericton, N.B., Canada E3B 5A3

(*Received* 13 *July* 1992; *accepted in revised form* 2 *March* 1993)

Abstract—An investigation on vorticity in general heterogeneous and non-steady flows is presented. The bulk vorticity of a flow is solely determined by the imposed boundary conditions and it exerts no constraints on local flow. The distribution of bulk vorticity in different rheological domains and the partitioning of the distributed vorticity into shear-induced vorticity and spin are both time dependent. This indicates that heterogeneous flows are inevitably non-steady. In a quantitative example, it is demonstrated that even though the imposed boundary movement is a constant simple shear, local flow can be non-steady, spinning and non-coaxial. Super-simple shear flow with internal kinematic vorticity number greater than 1 occurs, but the finite strain does not necessarily pulsate. The geological implications of this investigation are discussed. The significance of heterogeneity and non-steadiness in natural deformations are emphasized. It is concluded that vorticity distribution and partitioning is the link between different scale structures. The internal kinematic vorticity number is not a criterion of finite strain oscillation.

INTRODUCTION

ALTHOUGH it is common knowledge for structural geologists that natural deformations are generally heterogeneous and non-steady, simple and unique relationships between bulk and local strains (and for finite and instantaneous strains) in the idealized flows studied by, for example, Ramsay & Graham (1970), Elliott (1972), Ramberg (1975), Ramsay (1980), Ramsay & Huber (1983) are often implicitly or explicitly assumed in the study of natural deformation. To directly relate a hand specimen or even thin-section-scale shear-sense indicator to the bulk kinematics is an example. However, many geologists have provided evidence to challenge this practice. For example, Mitra (1976, 1978) has shown that the finite strain may be independent of the instantaneous strain rate. He defined a parameter called *strain activity* to measure the time-averaged instantaneous strain rate. Williams & Schoneveld (1981) concluded that garnet rotation is not related to the bulk strain path but only related to the movement of the 'particles' in contact with it. Lister & Williams (1979, 1983) have theoretically shown and provided observed evidence to emphasize that local flow may deviate significantly from bulk flow. Celma (1982) has shown that even at the scale of a thin-section, domains in which a fabric study gives an opposite sense of shear to that deduced from other field evidence may be found to coexist with domains in which the fabric is in agreement with the regional sense of shear. From the asymmetric quartz fabric in their shear zones, Platt & Behrmann (1986) also concluded that large volumes of rocks in shear zones may deform nearly coaxially and fail to reflect the bulk sense of shear. These examples all suggest the heterogeneous and time-dependent distribution of strain rates and vorticity in deformation history. Heterogeneous distribution of strain rates is well reflected by the finite strain variation in deformed rocks. In order to understand the deformation path, we are concerned not so much about the strain rates as about the non-coaxiality of the flow, sense of shear and whether reverse sense of shear has ever occurred. In such a case, vorticity analysis is very important. While many aspects of vorticity and their geological implications have been studied (Means *et al.* 1980, Lister & Williams 1983, Passchier 1986, 1990), a treatment of vorticity in general heterogeneous and non-steady flows is still absent. This paper serves to fill this vacancy. It will show what determines the bulk vorticity, how the bulk vorticity is distributed in different domains, how the distributed vorticity can be partitioned, and why the distribution and partitioning of vorticity are important in the study of natural deformation. Since an infinite variety of heterogeneous and non-steady flow examples can be considered, this paper will attempt to elucidate some general principles.

DESCRIPTION OF FLOW

A flow is totally defined if the velocity of all particles at any time is defined. The velocity can be expressed either in terms of particle (**X**)—Lagrangian or material velocity—or in terms of spatial location (**x**)—Eulerian or spatial velocity (Ottino 1989), i.e.:

$$\mathbf{v} = \mathbf{v}(\mathbf{X}, t) \quad \text{Lagrangian or material}$$

$$\mathbf{v} = \mathbf{v}(\mathbf{x}, t) \quad \text{Eulerian or spatial.}$$

The material derivative of **v**, $D\mathbf{v}/Dt$—the acceleration of particle **X**—is related to the spatial derivative of **v**, $\partial\mathbf{v}/\partial t$—the change of velocity at the spatial location **x**—as (*ibid.*):

$$\frac{D\mathbf{v}}{Dt} = \frac{\partial \mathbf{v}}{\partial t} + \mathbf{L} \cdot \mathbf{v}, \tag{1}$$

where **L** is the Eulerian velocity gradient tensor whose components are:

$$L_{ij} = \frac{\partial v_i}{\partial x_j} \quad (i, j = 1, 2, 3). \tag{2}$$

To distinguish Lagrangian velocity from Eulerian velocity is important in the subsequent establishment of the 'principle of bulk vorticity determination'. If $D\mathbf{v}/Dt = 0$, the flow is rigid-body translation, whereas $\partial \mathbf{v}/\partial t = 0$ means that the flow is steady. However at flow boundaries $D\mathbf{v}/Dt = 0$ means the boundary movement condition does not change with time. This may be common.

A flow is equally defined if the deformation history—the deformation gradient tensor $\mathbf{F}(t)$—at any time is defined. $\mathbf{F}(t)$ and $\mathbf{L}(t)$ are related as (Truesdell 1965, pp. 19–20):

$$\mathbf{L}(t) = \dot{\mathbf{F}}(t)\mathbf{F}^{-1}(t). \tag{3}$$

L can be decomposed into a symmetric stretching tensor **D** and an antisymmetric vorticity tensor **W** (Truesdell 1965, Means *et al.* 1980):

$$\mathbf{L} = \mathbf{D} + \mathbf{W}. \tag{4}$$

Vorticity tensor can be expressed in terms of the vorticity vector (see Means *et al.* 1980, Passchier 1986). In this paper the vector notation of vorticity is used.

If **L** does not vary from point to point, the flow is homogeneous, otherwise it is heterogeneous. In the case of heterogeneous flow, the variation of vorticity in space is called distribution in this paper. If **L** does not change with time, the flow is steady, otherwise it is non-steady.

A dimensionless magnitude—kinematic vorticity number—was defined by Truesdell (1954) as:

$$W_k = W \cdot \{2(s_1^2 + s_2^2 + s_3^2)\}^{-1/2}, \tag{5}$$

where W is the vorticity, and s_1, s_2, s_3, are the principal instantaneous stretching rates. $W_k = 0$ corresponds to purely irrotational flow and $W_k = \infty$ corresponds to purely rotational flow (Truesdell 1954).

It was recognized by Means *et al.* (1980) and Lister & Williams (1983) that vorticity can be partitioned into a frame-independent 'internal' or shear-induced vorticity (rotation of material lines with respect to the instantaneous stretching axis) and a frame-dependent 'external' vorticity or spin (rotation of the instantaneous stretching axis with respect to the external frame), i.e.:

$$W = \text{SIV} + \text{spin}.$$

The internal kinematic vorticity number defined by Means *et al.* (1980) as

$$W_k' = \text{SIV} \cdot \{2(s_1^2 + s_2^2 + s_3^2)\}^{-1/2} \tag{6}$$

is a measure of the degree of instantaneous non-coaxiality. $W_k' = 0$ is the only type of coaxial flow; $0 < W_k' < 1$ the flow is sub-simple shear; $W_k' = 1$ is simple shear and $W_k' > 1$ is super-simple shear.

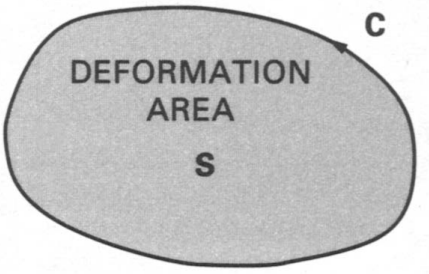

Fig. 1. A deformation area **S** with **C** as its boundary. Boundary conditions defined by $\int_C \mathbf{v} \cdot d\mathbf{x}$ determines the vorticity flux through **S** and thus establish the bulk vorticity of the deformation (equation 11). In the process of deformation **S** and **C** may change. The change of bulk vorticity is described by equation (12). See text for detail.

THE DETERMINATION OF BULK VORTICITY

Mathematically, vorticity vector is the curl of the velocity field defined as:

$$\mathbf{W} = \text{curl}\,\mathbf{v} = \lim_{S \to 0} \frac{\oint_C \mathbf{v}\, d\mathbf{x}}{\int_S d\mathbf{S}} = \left(\mathbf{i}\frac{\partial}{\partial x_1} + \mathbf{j}\frac{\partial}{\partial x_2} + \mathbf{k}\frac{\partial}{\partial x_3}\right) \times \mathbf{v}. \tag{7}$$

According to Stokes's curl theorem:

$$\int_S \text{curl}\,\mathbf{v}\, d\mathbf{S} = \oint_C \mathbf{v}\, d\mathbf{x}, \tag{8}$$

where **S** is any area that has **C** as its boundary, the left-hand side being the vorticity flux of the area **S** and the right-hand side being the circulation of **v** along **C**, the instantaneous average vorticity through the area **S** is:

$$W = \frac{1}{S}\int_S \text{curl}\,\mathbf{v}\, d\mathbf{S} = \frac{1}{S}\oint_C \mathbf{v}\, d\mathbf{x}, \tag{9}$$

where S is the area of **S**.

Since (8) holds for any loop **C**, choosing a particular **C** which is exactly the material boundary of the flow (Fig. 1), the whole vorticity flux of the flow is:

$$\int_S \mathbf{W}\, d\mathbf{S} = \oint_C \mathbf{v}\, d\mathbf{x}. \tag{10}$$

The bulk vorticity (W_b) of the flow is thus:

$$W_b = \frac{1}{S}\oint_C \mathbf{v}\, d\mathbf{x}. \tag{11}$$

where S is the whole area and **C** is the material boundary of the flow. As flow advances, the area S and the boundary **C** vary with time. The variation of W_b with respect to time is (see Appendix A):

$$\frac{dW_b}{dt} = \frac{1}{S}\oint_C \left(\frac{D\mathbf{v}}{Dt} - \frac{\partial \ln S}{\partial t}\mathbf{v}\right) d\mathbf{x}. \tag{12}$$

The terms on the right-hand sides of equations (11) and (12) are all boundary movement conditions. Therefore: *the bulk vorticity of a flow is solely determined by the imposed boundary movements; its change with time is*

dependent only on the boundary movement and bulk area changes; bulk vorticity is independent of the way in which the deformation is accommodated. Since this states the relationship between local flow and bulk flow, I wish to call it *the principle of bulk vorticity determination.*

If $D\mathbf{v}/Dt = 0$ along $\mathbf{C}$, by solving (12) incorporating (11) we have (see Appendix A):

$$W_b S = \text{constant}. \tag{13}$$

It means if boundary movement remains unchanged, the bulk vorticity flux is conserved.

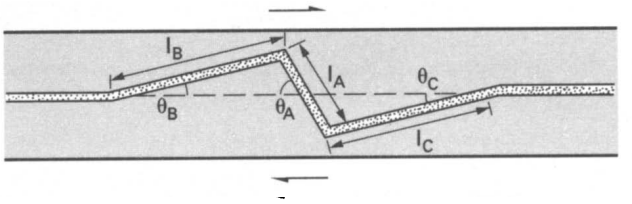

Fig. 3. In a shear zone, before the initiation of drag fold, the bulk vorticity is distributed in incompetent domains, while the competent layer has nearly no vorticity. When drag fold is initiated, the bulk and vorticity is redistributed. The competent layer takes up some vorticity the vorticity in the incompetent matrix is correspondingly reduced. The distribution of vorticity changes with time. See text for detail.

THE DISTRIBUTION OF VORTICITY IN HETEROGENEOUS FLOW

In homogeneous flow, the vorticity is uniformly distributed. The vorticity at any point of the flow equals the bulk vorticity.

When the material of the flow is rheologically heterogeneous, the vorticity varies in space. However, as is the common practice in structural geology, the flow can be divided into many approximately homogeneous domains. In each domain, the vorticity can be approximately viewed as uniform. Therefore a heterogeneous area $\mathbf{S}$ is divided into n subareas $\mathbf{S}_1, \mathbf{S}_2, \mathbf{S}_3, \ldots, \mathbf{S}_n$ (Fig. 2). The bulk vorticity is:

$$W_b = \frac{1}{S}\int_{\mathbf{S}} \mathbf{W}\,d\mathbf{S} = \frac{1}{S}\left(\int_{\mathbf{S}_1} \mathbf{W}\,d\mathbf{S} + \int_{\mathbf{S}_2} \mathbf{W}\,d\mathbf{S} + \int_{\mathbf{S}_3} \mathbf{W}\,d\mathbf{S} + \cdots + \int_{\mathbf{S}_n} \mathbf{W}\,d\mathbf{S}\right)$$

$$= \frac{1}{S}(S_1W_1 + S_2W_2 + S_3W_3 + \cdots + S_nW_n), \tag{14}$$

where S_i and W_i are the area and the average vorticity of the ith domain respectively, and $W_i = 1/S_i \int_{\mathbf{C}_i} \mathbf{v} \cdot d\mathbf{x}$, where $\mathbf{C}_i$ is the boundary of the ith domain. Equation (14) may be written as

$$W = \Sigma \lambda_i W_i, \tag{15}$$

where λ_i is the area percentage of the ith domain in the flow area and $\Sigma \lambda_i = 1$. Equation (15) specifies the way in which the bulk vorticity determined by the imposed boundary conditions of the flow is distributed in different domains. Several specific situations are now reviewed to demonstrate the effect of vorticity distribution.

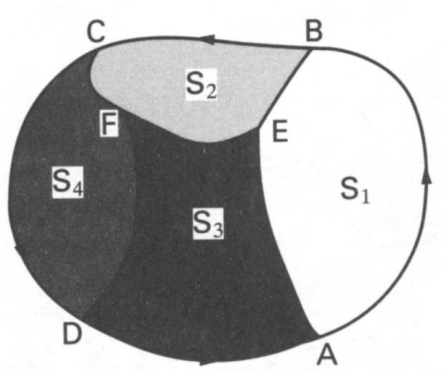

Fig. 2. A heterogeneous deformation is divided into several approximately homogeneous domains. For each domain, we have: $\int_{S_i} \mathbf{W}_i \cdot d\mathbf{S} = \int_{C_i} \mathbf{v} \cdot d\mathbf{x}$ where $\mathbf{C}_1$ = ABEA, $\mathbf{C}_2$ = BCFEB, etc. In the process of deformation there are continual vorticity exchange between domains leading to non-steady flow in different domains.

Drag fold development in a shear zone

In a shear zone undergoing simple shear where a competent layer is parallel to the flow plane as shown in Fig. 3, before the initiation of folding, the bulk vorticity is distributed such that the competent layer takes nearly zero vorticity while the vorticity of the incompetent layers is larger than the bulk vorticity, since according to equation (14), we have:

$$\mathbf{W}_b(S_i + S_c) = W_iS_i$$

$$W_i = (1 + R)W_b, \tag{16}$$

where R is the ratio of the area of the competent layer S_c to that of the incompetent layer S_i (hereafter R is referred to as the heterogeneity factor in this paper). There is a very strong vorticity gradient across the competency contrast boundary. As flow advances, there is a strong tendency for the competent layers to take up some of the vorticity by spinning as suggested by Lister & Williams (1983).

Imagining some variation in strength properties causes the area l_A to spin, the adjacent areas l_B and l_C will be forced to rotate in the opposite sense (Fig. 3), we have:

$$l_A \sin\theta_A = l_B \sin\theta_B + l_C \sin\theta_C. \tag{17}$$

Differentiating (17), after arrangement, we have:

$$\frac{d\theta_A}{dt} = \frac{l_B \cos\theta_B}{l_A \cos\theta_A}\frac{d\theta_B}{dt} + \frac{l_C}{l_A}\frac{\cos\theta_C}{\cos\theta_A}\frac{d\theta_C}{dt} \qquad (\theta_A \neq 90°)$$

$$l_B \cos\theta_B \frac{d\theta_B}{dt} + l_C \cos\theta_C \frac{d\theta_C}{dt} = 0 \qquad (\theta_A = 90°). \tag{18}$$

The incremental vorticity of the competent layer is:

$$\Delta W = \frac{2l_A \frac{d\theta_A}{dt} - 2l_B \frac{d\theta_B}{dt} - 2l_C \frac{d\theta_C}{dt}}{l_A + l_B + l_C} \quad (19a)$$

when $\theta_A \neq 90°$, after arrangement:

$$\Delta W = 2\frac{\frac{d\theta_B}{dt} l_B\left(\frac{\cos\theta_B}{\cos\theta_A} - 1\right) + \frac{d\theta_C}{dt} l_C\left(\frac{\cos\theta_C}{\cos\theta_A} - 1\right)}{l_A + l_B + l_C}$$

$$(\theta_A \neq 90°). \quad (19b)$$

When $\theta_A < 90°$, $d\theta_B/dt$ and $d\theta_C/dt > 0$, and since $\theta_A > \theta_B$ or θ_C, from (19b) $\Delta W > 0$. When $\theta_A \geq 90°$, areas l_B and l_C will rotate in the same sense as l_A, i.e. $d\theta_B/dt$ and $d\theta_C/dt < 0$, from (19a), still $\Delta W > 0$. Therefore (19) is always positive. This indicates that the competent layer, by initiating folding, takes on some of the vorticity and the vorticity of the incompetent matrix decreases correspondingly. The vorticity gradient across the competent–incompetent boundary is reduced. As flow develops, the distribution of vorticity changes as is indicated in equation (19) since θ changes with time.

Rotation of rigid inclusions in ductile matrix

The angular velocity (ω) of a rigid elliptical inclusion with an aspect ratio N in a zone of simultaneous combination of simple shear ($\dot{\gamma}$) and pure shear ($\dot{\varepsilon}$) is given by Ghosh & Ramberg (1976, equation 3)

$$\omega = 1/(N^2 + 1)[\dot{\gamma}(N^2\cos^2\phi + \sin^2\phi) + \dot{\varepsilon}(N^2 - 1)\sin 2\phi], \quad (20)$$

where ϕ is the instantaneous angle of the long axis of the inclusion with respect to the flow plane.

The variation of ω as ϕ changes is shown in figs. 2 and 3 of Ghosh & Ramberg (1976). For any N, $\dot{\gamma}$ and $\dot{\varepsilon}$ the average magnitude of ω over 0–180° is always $0.5\dot{\gamma}$. The average vorticity of the inclusions equals the bulk vorticity. However, in the process of rotation the vorticity of the inclusion varies. This means that there is continual redistribution of vorticity between the inclusions and the matrix.

In the study of garnet rotation by Williams & Schoneveld (1981), perfect coupling requires that the angular velocity of garnets equals the shear strain rate. In such a case,

$$W_b(S_g + S_m) = W_g S_g + W_m S_m, \quad (21)$$

where W_b is the bulk vorticity ($W_b = \dot{\gamma}$); W_g is the vorticity (spin) of garnet ($W_g = 2\dot{\gamma}$); W_m, S_m, S_g are the vorticity of matrix, area of matrix and area of garnet, respectively. Therefore:

$$W_m = \dot{\gamma}(1 - S_g/S_m) < \dot{\gamma}. \quad (22)$$

It is readily seen that if garnets rotate in the suggested model, then the matrix will have less vorticity ($W_m < \dot{\gamma}$). However if discontinuous slip takes place along the garnet–matrix contact, this slip can take up large amounts of vorticity flux and serves as a means to accommodate vorticity difference.

Shear zones cutting layers with competency heterogeneity

Consider a shear zone cutting layers with competency heterogeneity as in Fig. 4, for example, a thrust or extensional fault cutting a sedimentary sequence. Suppose the layers are at an arbitary angle ϕ with respect to x_2 (shear zone normal). As has been observed by Lister & Williams (1983) the competent layer tends to spin and keep the local flow as coaxial as possible, whereas the incompetent layer will undergo non-coaxial flow by strain compatibility. If the boundary movement is simple shear with a strain rate $\dot{\gamma}$ then the velocity field is:

$$v_1 = dx_1/dt = \dot{\gamma}x_2$$

$$v_2 = dx_2/dt = 0 \quad (23)$$

$$\tan\phi = x_1/x_2. \quad (24)$$

Differentiating (24) and incorporating (23) gives:

$$d\phi/dt = \dot{\gamma}\cos^2\phi.$$

Therefore the vorticity of the competent layer W_c is

$$W_c = 2\dot{\gamma}\cos^2\phi. \quad (25)$$

According to equation (14) the average vorticity of the incompetent layer W_i and the areas of competent layer and incompetent matrix S_c and S_i are related as:

$$\dot{\gamma}(S_i + S_c) = 2\dot{\gamma}\cos^2\phi S_c + W_i S_i$$

or

$$W_i = \dot{\gamma}(1 - R\cos 2\phi), \quad (26)$$

where R is the local heterogeneity factor.

Obviously, if $S_c \ll S_i$, $W_i \approx \dot{\gamma}$.

The deformation history of incompetent layer and the non-coaxiality of the flow is investigated later in the paper.

Discontinuous slip planes

Stokes's curl theorem can be used to extend the concept of vorticity to situations where discontinuities

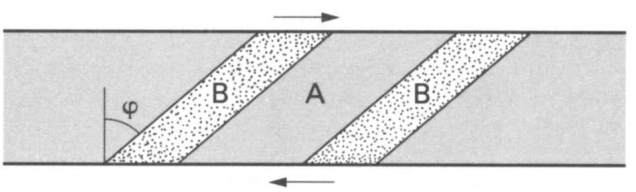

Fig. 4. Shear zone with rheologically heterogeneous layers at an arbitary angle ϕ with respect to the shear zone boundary normal. A and B are incompetent and competent layers, respectively. B domain tries to keep the local flow as coaxial as possible whereas A domain undergoes non-coaxial flow (see Lister & Williams 1983 for discussion). Because of vorticity distribution and partitioning, the deformation path of domain A is a non-steady spinning non-coaxial flow; super-simple shear ($W_k' > 1$) occurs and if $R > 0.41$, reverse sense of shear occurs. See text for detail.

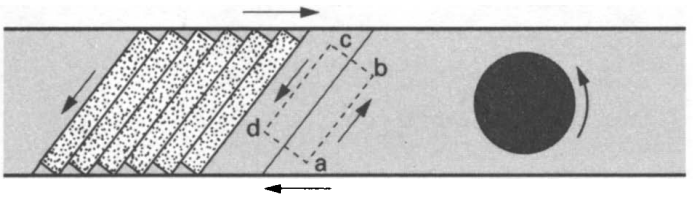

Fig. 5. Slip on discontinuous planes such as foliations or competency contrast boundaries like those between garnet and matrix can accommodate large amounts of vorticity flux. Here the bulk vorticity determined by shear zone boundary movement is $\dot{\gamma}$. The vorticity of the rock between slip planes is $2\dot{\gamma}\cos^2\phi$, whereas the vorticity of garnet, when perfectly coupling (see Williams & Schoneveld 1981) is $2\dot{\gamma}$. The vorticity differences are balanced by slip on discontinuous planes. Discontinuous slip can contribute to local flow non-steadiness. See text for detail.

develop. For a discontinuous plane initiated in a shear zone (Fig. 5), slip on the plane would contribute a uniform translation component to the velocity field. Suppose the relative velocity of displacement of the plane is v. For the loop C ($abcd$) as in Fig. 5, we have:

$$\int_S \text{curl } \mathbf{v}\, d\mathbf{S} = \oint_C \mathbf{v}\, d\mathbf{x} = \frac{v}{w}, \tag{27}$$

where w is the width of the loop. Obviously this vorticity is accommodated by the movement on the plane, since by narrowing the loop, the vorticity magnitude becomes larger, until when $w \to 0$, $W \to \infty$. If the slip planes are penetrative as C or C' planes in shear zones, the average vorticity accommodated by them would be

$$W_s = 1/w \sum v_i = v_a/d, \tag{28}$$

where W_s is the average slip plane accommodated vorticity, v_a is the average slip velocity on slip planes and d is average spacing of slip planes.

Therefore if slip on discontinuous planes is considered, the bulk vorticity is decomposed into W_{con} (vorticity of continuous domains between slip planes) and W_s (vorticity due to slip on discontinuous planes), we have

$$W = W_s + W_{con}. \tag{29}$$

If W_s is significant, W_{con} can be greatly different from the bulk vorticity. It is readily seen that discontinuous slip can contribute to the deviation of local flow from bulk flow because it makes great vorticity difference between adjacent domains possible.

A QUANTITATIVE EXAMPLE OF VORTICITY PARTITIONING

At any instant, the distributed vorticity in a particular domain is partitioned into shear-induced vorticity and spin. In this section, the example shown in Fig. 4 is used to show how the distributed vorticity can be partitioned.

The vorticity distributed in the competent layer is accommodated by spin, so the problem is how vorticity partitioning takes place in the incompetent layer. In order to examine this problem a reference frame is established (Fig. 6) with x_1 parallel to the bulk shear zone boundary, x_2 normal to the shear zone. $A_0B_0C_0D_0$, $E_0F_0G_0H_0$, ABCD and EFGH are segments of competent layers which exhibit spinning coaxial deformation. $A_0D_0G_0F_0$, ADGF are segments of incompetent layers. Figure 6(a) corresponds to the 0-configuration ($\phi = 0$) and Fig. 6(b) corresponds to the ϕ-configuration ($\phi \neq 0$) M_0,N_0Q_0,R_0 and M,N,Q,R are mid-points of A_0B_0, C_0D_0, E_0F_0, G_0H_0, etc. If the two competent layers enclosing the incompetent area are symmetrical then the origin of the frame is chosen to be at the mid-point of A_0F_0 as in Fig. 6(b), otherwise the origin is placed where QM intersects x_1.

If the reference configuration is the 0-configuration, the deformation equations at any time t are (see Appendix B):

$$x_1 = [1 + R(2 + R)\sin^2\phi]^{1/2}\cos\beta x_1^0 + \tan\phi x_2^0$$
$$x_2 = [1 + R(2 + R)\sin^2\phi]^{1/2}\sin\beta x_1^0 + x_2^0, \tag{30}$$

where $\beta = \tan^{-1}[R\sin\phi\cos\phi/(1 + R\sin^2\phi)]$, ϕ is the angle of the competent layers with respect to the shear zone normal at the deformed state (ϕ-configuration) and is a function of t. R is the local heterogeneity factor.

The deformation gradient tensor of the incompetent layer $\mathbf{F}$ which is a function of t is thus:

$$\mathbf{F}(t) = \begin{bmatrix} \mathbf{A}\cos\beta & \tan\phi \\ \mathbf{A}\sin\beta & 1 \end{bmatrix}, \tag{31}$$

where $\mathbf{A} = [1+R(2 + R)\sin^2\phi]^{1/2}$.

If the reference configuration is defined when the

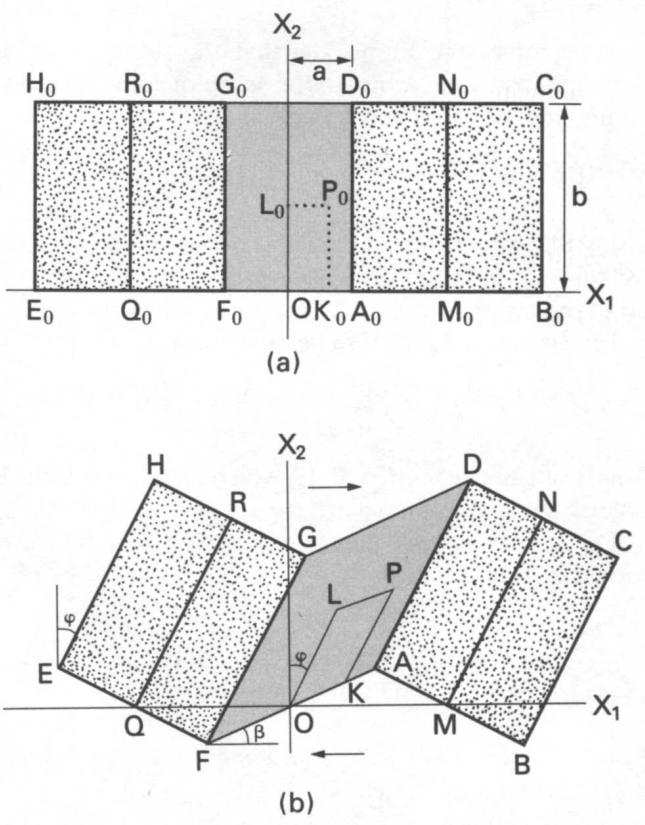

Fig. 6. External reference frame fixed to the boundary of the shear zone for the derivation of the deformation tensor of the incompetent layers. (a) 0-configuration; (b) ϕ-configuration.

competent layers are at an initial angle ϕ_0 with respect to shear zone normal (ϕ_0-configuration), the deformation tensor $\mathbf{F}_{\phi_0}$ is (see Appendix B):

$$\mathbf{F}_{\varphi_0}(t) = \begin{bmatrix} \mathbf{A}\cos\beta & \tan\varphi \\ \mathbf{A}\sin\beta & 1 \end{bmatrix} \begin{bmatrix} 1 & -\tan\varphi_o \\ -\mathbf{A}_0\sin\beta_0 & \mathbf{A}_0\cos\beta_o \end{bmatrix}, \tag{32}$$

where $\mathbf{A}_0 = [1 + R(2 + R)\sin^2\phi_0]^{1/2}$, $\beta_0 = \tan^{-1}[R\sin\phi_0\cos\phi_0/(1 + R\sin^2\phi_0)]$.

From equation (3), the velocity gradient tensor $\mathbf{L}(t)$ is:

$$\mathbf{L}(t) = \dot{\mathbf{F}}_{\varphi_0}(t)\mathbf{F}_{\varphi_0}^{-1} = \begin{bmatrix} \dot{\mathbf{A}}\cos\beta - \mathbf{A}\sin\beta\dot{\beta} & \dot{\gamma} \\ \dot{\mathbf{A}}\sin\beta + \mathbf{A}\cos\beta\dot{\beta} & 0 \end{bmatrix} \begin{bmatrix} 1 & -\tan\varphi \\ -\mathbf{A}\sin\beta & \mathbf{A}\cos\beta \end{bmatrix}, \tag{33}$$

where $\dot{}$ means differentiation with respect to t.

The *left Cauchy-Green tensor* **B** (for definition, the reader is referred to Truesdell 1965) is:

$$\mathbf{B} = \mathbf{F}_{\phi_0}\mathbf{F}_{\phi_0}^{\mathrm{T}}. \tag{34}$$

From equation (33), the angle of the principal instantaneous stretching axis with respect to x_1 (θ_i), principal instantaneous stretching rates (s_1, s_2) and the instantaneous vorticity can be calculated (see Truesdell 1965, Means *et al.* 1980, Passchier 1986). From equation (34), finite principal stretches can be calculated at different t for given R, ϕ_0. The spin of the instantaneous stretching axis is:

$$\text{spin} = -2\frac{d\theta_i}{dt} = -2\frac{d\theta_i}{d\varphi}\frac{d\varphi}{dt} = -2\cos^2\varphi\frac{d\theta_i}{d\varphi} \approx -2\cos^2\varphi\frac{\Delta\theta_i}{\Delta\varphi}.$$

The negative sign represents that the decrease of θ_i corresponds to the sympathetic sense of spin. The SIV component of the vorticity is thus:

$$\text{SIV} = W_i - \text{spin} = 2\cos^2\varphi\frac{d\theta_i}{d\varphi} - R\cos 2\varphi + 1.$$

Using SIV and principal instantaneous stretching rates, we can obtain the internal kinematic vorticity number (W_k') (equation 3).

The condition for SIV to be always positive is:

$$\text{SIV}|_{\varphi=0} = 2\left.\frac{d\theta_i}{d\varphi}\right|_{\varphi=0} - R + 1 \geq 0.$$

This is satisfied when $R \leq 0.41$, which means if $R \leq 0.41$ reverse shear will not occur.

The results of the above presented calculation are shown in Figs. 7–12.

DISCUSSION AND GEOLOGICAL IMPLICATIONS

Vorticity distribution and partitioning: the bridge to connect different scale structures

In understanding the development of structures of an area from the point of view of its kinematics, the geologist is faced with integrating observations on different scales. As pointed out by Hobbs *et al.* (1976), the most important difference between different scales is not simply the size of the area observed but the way in which the observation is made. From smaller scale to larger scale, interpretation is always involved.

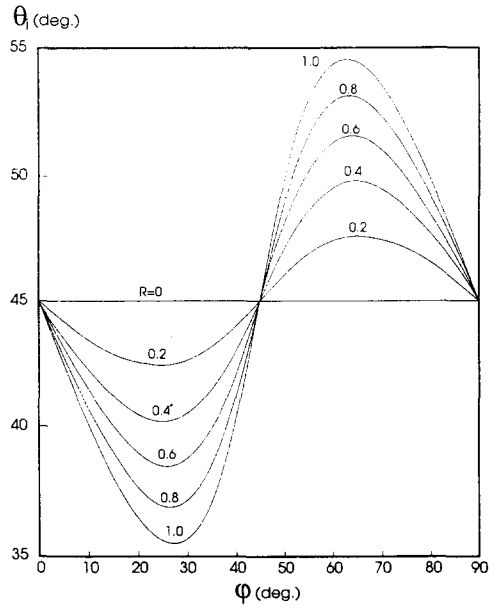

Fig. 7. Variation of the orientation of the principal instantaneous stretching axis (θ_i) vs the instantaneous orientation of the layers (ϕ) (the curves are symmetric about the vertical axis, so the variation from $-90°$ to $0°$ is omitted in this and subsequent figures). The instantaneous stretching axis is not fixed unless $R = 0$.

The principle of bulk vorticity determination shows that the bulk vorticity does not exert any constraints on local flow. In the quantitative model, although the imposed boundary displacement is a constant simple shear (bulk flow), the complexity of deformation path of the incompetent layer (local flow) is explicitly demon-

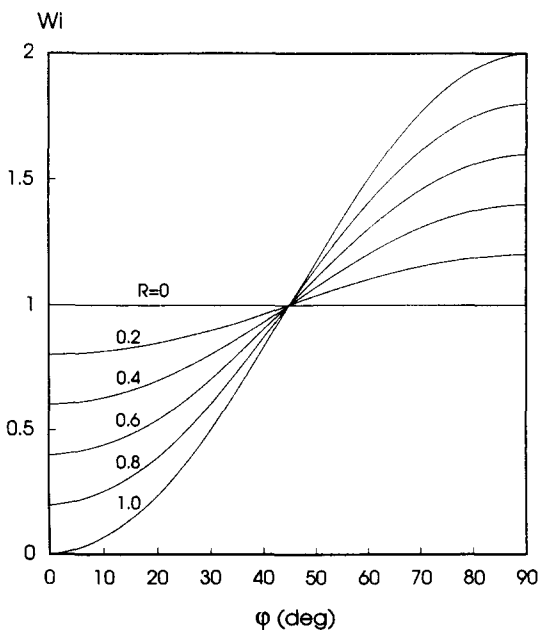

Fig. 8. Variation of the distributed vorticity in the incompetent layer (W_i) vs ϕ for different R (the bulk shear strain rate is set at 1, otherwise the vertical axis should be $W_i/\dot{\gamma}$).

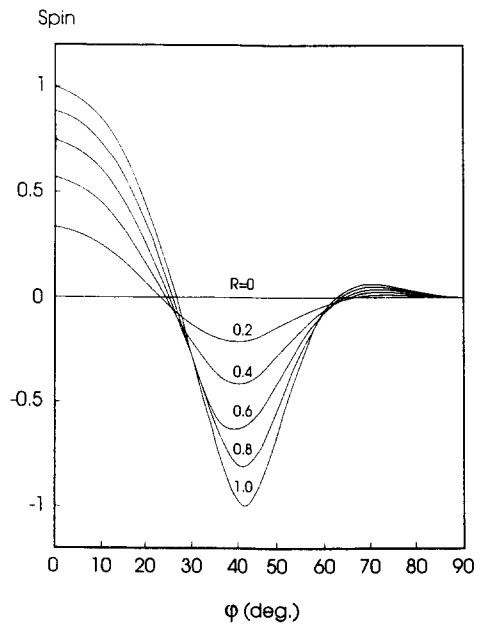

Fig. 9. Variation of the spin component of W_i vs ϕ for different R. For different ϕ, spin may be sympathetic (>0) or antithetic (<0).

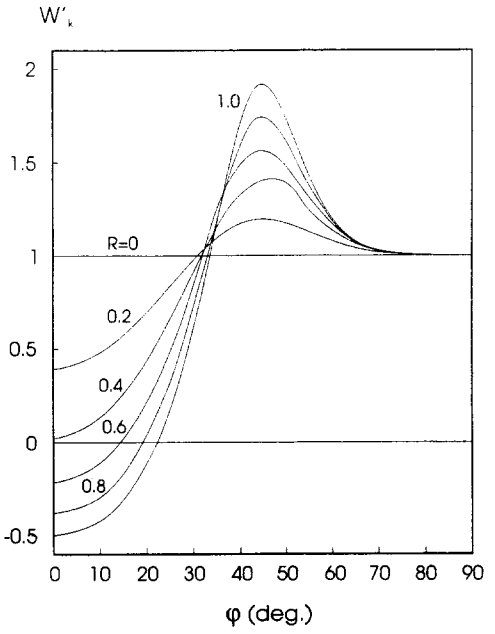

Fig. 11. Variation of the internal kinematic vorticity number (W_k') vs ϕ for different R. There is always a range around ±45° where $W_k' > 1$. W_k' is maximum at $\phi = \pm 45°$.

strated in Figs. 7–12. It can undergo reverse (SIV < 0) shear (if the local $R > 0.41$), forward shear (SIV > 0) or instantaneously coaxial (SIV = 0) depending on the instantaneous angle ϕ. The larger the magnitude of R, the wider the range in which reverse shear can occur (Fig. 10). As ϕ approaches 90°, the flow approaches simple shear (Figs. 7–12). Therefore it can be concluded that the more heterogeneous the rocks, the more likely kinematically inconsistent structures will develop; whereas the higher the finite strain, the more likely we will see kinematically consistent structures.

In the quantitative model, the instantaneous stretching axis keeps spinning sympathetically or antithetically depending on the instantaneous ϕ (Fig. 9). The flow is obviously non-steady, spinning and non-coaxial. In natural shear zones, R may vary from domain to domain and with time due to strain softening or hardening, development of fabrics, growth of new minerals, change of thermodynamic conditions, etc. One can instantly imagine how complex the structural evolution in nature can be. Even the finite strain, which is generally considered to be relatively easy to deal with, is dependent on the deformation history: the finite strain of the incompetent layer (local finite strain ε_{LF}) is a complicated function of the initial angle ϕ_0, local rheological heterogeneity factor R and the bulk finite strain (ε_{BF}) which can be expressed as:

$$\varepsilon_{LF} = f(\phi_0, R, \varepsilon_{BF}). \quad (35)$$

Even from strain measurement, if we obtain ε_{LF}, in order to get ε_{BF} we must know the original configuration ϕ_0 and the rheological heterogeneity factor R, which may be a function of many factors operating in the history of the deformation. Unless we know or assume ϕ_0 and R, no inference of ε_{BF} from ε_{LF} can be reasonably made. It follows from the above that there are no simple and unique relationships between bulk and local strains, finite and instantaneous strains. To establish the bulk kinematics from the combination of local observations, understanding the distribution and partitioning of the bulk vorticity is a necessity. The assumption that simple deformation mechanisms such as simple shear are invoked for all scales of rock deformation (e.g. Mattauer 1975, 1986, Bird 1978, Brunel 1986) cannot be justified.

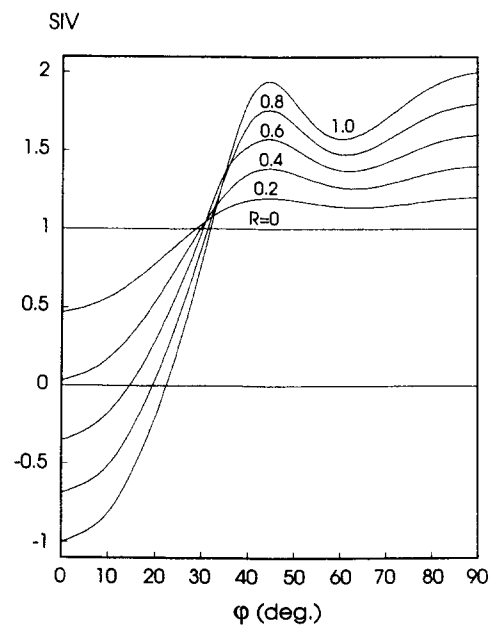

Fig. 10. Variation of the SIV component of W_i vs ϕ for different R. If $R \leq 0.41$ then SIV is always positive. When $R > 0.41$, reverse sense of shear occurs and it is maximum at $\phi = 0$. SIV reaches its maximum forward shear at $\phi = \pm 45°$ then after a decrease reaches its maximum again at $\phi = \pm 90°$.

The non-steadiness of natural deformations

All situations of vorticity distribution studied indicate that the distribution is a function of time. Since the bulk

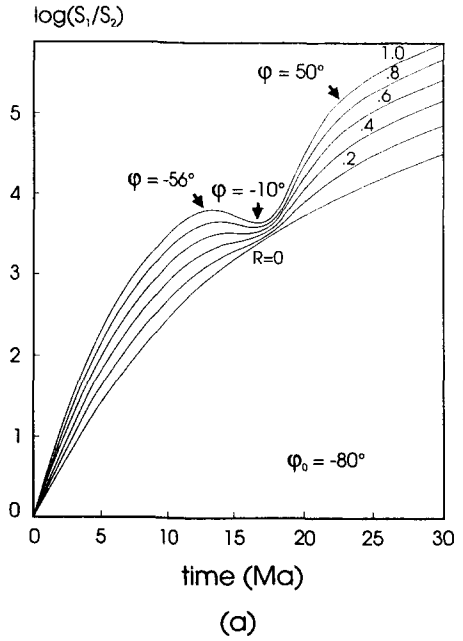

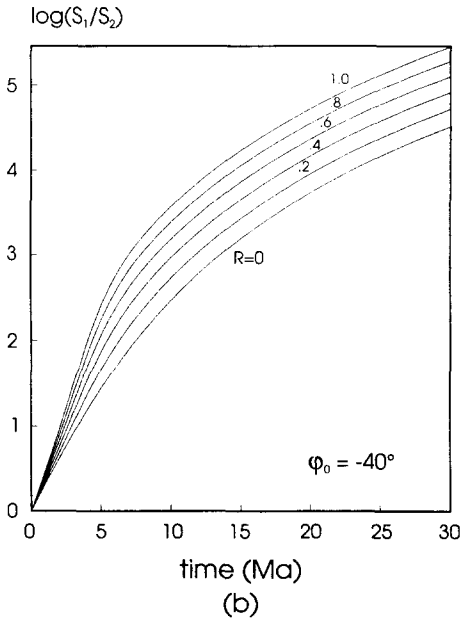

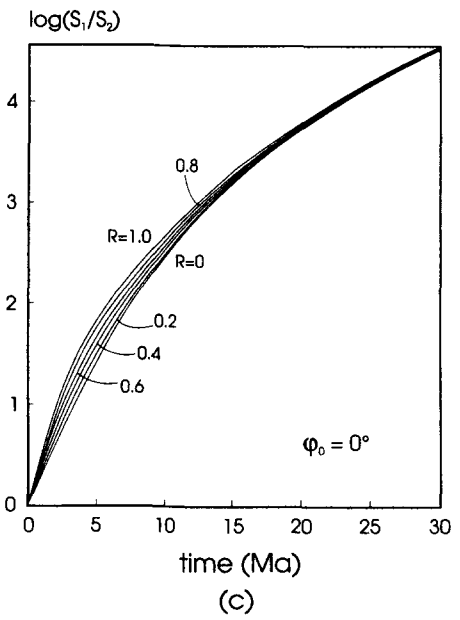

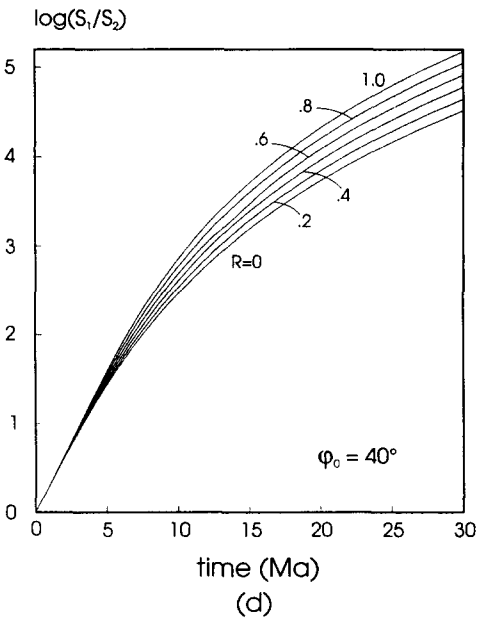

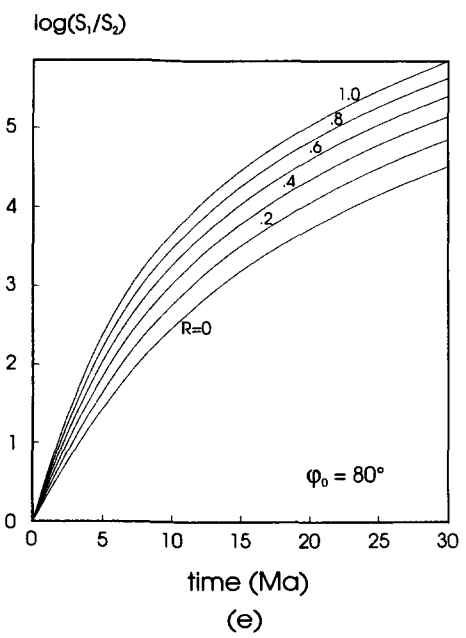

Fig. 12. Plot of logarithm of the ratio of the maximum to minimum principal stretches against time for the deformation history of the incompetent domain for different ϕ_0 and local heterogeneity factor R. $R = 0$ corresponds to bulk progressive simple shear. The bulk shear strain rate is set at $10^{-14}s^{-1}$. Although $W_k' > 1$ occurs for any R, the finite strain pulsates only in the event $\phi_0 = -80°$ (a). In this case, the oscillation occurs in the range of ϕ as indicated by arrows in which W_k' may vary significantly (compare to Fig. 11). No correspondence exists between the magnitude of W_k' and finite strain oscillation.

vorticity and its change with time are independently determined by the boundary movement, it is unlikely that the bulk vorticity will change in such a way as to keep the distributed vorticity in each domain steady. It follows that the deformation path in different domains is, in general, time-dependent, so long as rheological heterogeneity exists. Therefore heterogeneous flow is also non-steady. Homogeneous and/or steady flows will only occur where strain softening is so complete that rheological heterogeneity vanishes. This is only possible locally and over relatively short periods of time where vorticity redistribution can be neglected.

Successive development of folds in ductile shear zones has been aptly interpreted as a result of local flow field perturbance caused by 'islands' of rigid or less deformed units as porphyroclasts, pebbles or boudins (Hudleston 1977, 1989, Bell 1978, Cobbold & Quinquis 1980), variation in strength properties (Lister & Williams 1983) or mechanical heterogeneity induced instability (Ghosh & Sengupta 1984, 1987). Platt (1983) points out that there are variations of vorticity partitioning along the foliation which may offer an alternative interpretation: an increase in shear-induced vorticity would cause backward spins which do not amplify, whereas a decrease in SIV would cause forward spins which amplify. However, when we look into the reasons for such variations of vorticity partitioning, we have to return to local flow field perturbances caused by material heterogeneity. Even when the material is more or less homogeneous, differences of strain softening and/or hardening are always expected which could induce rheological heterogeneity and hence local flow non-steadiness.

Shortened or folded boudins in nature have been interpreted either as the result of area change during progressive non-coaxial deformation at near simple shear flow conditions (e.g. Von Burns & Talbot 1986, Passchier 1990) or as due to two separate phases of deformation with different oriented principal shortening axis, each with $0 \leq W_k' \leq 1$ (Sengupta 1983, Passchier 1990). An alternative interpretation would be that boudinage results in local heterogeneity and leads to local non-steady flow.

Even in ductile regimes, discontinuous slip may occur at least transiently (Sibson 1977) on planes like foliations (e.g. Williams 1977). The present study shows that these slips can significantly contribute to local flow heterogeneity and non-steadiness because they make great vorticity differences between adjacent domains possible.

The internal kinematic vorticity number: not a criterion of finite strain oscillation

Sub- and super-simple shear have also been called non-pulsating and pulsating histories (Means *et al.* 1980). In the present model however, super-simple shear ($W_k' > 1$) occurs for any R (Fig. 11), but the finite strain does not pulsate except when $\phi_0 = -80°$ (Fig. 12). Even in this case, the finite strain oscillation does not correspond to $W_k' > 1$. Instead, W_k' varies significantly in the period of oscillation (compare Fig. 12a with Fig. 11).

Owing to non-steadiness, the finite strain may pulsate even for a coaxial flow ($W_k' = 0$). An obvious example is one with the instantaneous velocity field as:

$$v_1 = \cos t\, x_1,\ v_2 = -\cos t\, x_2. \tag{36}$$

The deformation gradient tensor is obviously:

$$\mathbf{F}(t) = \begin{bmatrix} \exp(\sin t) & 0 \\ 0 & \exp(-\sin t) \end{bmatrix}. \tag{37}$$

This flow is coaxial but the finite strain pulsates with a periodicity π. It is therefore clear that, for non-steady flow, W_k' can only specify the non-coaxility of the flow but not the oscillation of finite strain.

Acknowledgements—I am much grateful to Drs P. F. Williams and J. C. White for their encouragement, critically reading the early draft of the paper and offering valuable suggestions. I thank Drs J. G. Spray and A. Park for initiating discussion, Angel Gomez for assistance with figure preparation and Diane Tabor for assistance with word processing. Reviews by three anonymous referees have helped to improve the quality of the paper. The study is supported by Natural Sciences and Engineering Research Council of Canada (NSERC) operating grant A8512 to J. C. White.

REFERENCES

Bell, T. H. 1978. Progressive deformation and reorientation of fold axes in a ductile mylonite zone: the Woodroffe thrust. *Tectonophysics* **44**, 285–320.

Bird, P. 1978. Initiation of intracontinental subduction in the Himalaya. *J. geophys. Res.* **83**, 4975–4987.

Brunel, M. 1986. Ductile thrusting in the Himalayas: shear sense criteria and stretching lineations. *Tectonics* **5**, 247–265.

Celma, A. G. 1982. Domainal and fabric heterogeneities in the Cap de Creus quartz mylonites. *J. Struct. Geol.* **4**, 443–455.

Cobbold, P. R. & Quinquis, H. 1980. Development of sheath folds in shear regimes. *J. Struct. Geol.* **2**, 119–126.

Elliott, D. 1972. Deformation paths in structural geology. *Bull. geol. Soc. Am.* **83**, 2621–2638.

Ghosh, S. K. & Ramberg, H. 1976. Reorientation of inclusions by combination of pure shear and simple shear. *Tectonophysics* **34**, 1–70.

Ghosh, S. K. & Sengupta, S. 1984. Successive development of plane non-cylindrical folds in progressive deformation. *J. Struct. Geol.* **6**, 703–709.

Ghosh, S. K. & Sengupta, S. 1987. Progressive development of structures in a ductile shear zone. *J. Struct. Geol.* **9**, 277–289.

Hobbs, B. E., Means, W. D. & Williams, P. F. 1976. *An Outline of Structural Geology*. John Wiley, New York.

Hudleston, P. J. 1977. Similar folds, recumbent folds, and gravity tectonics in ice and rocks. *J. Geol.* **85**, 113–122.

Hudleston, P. J. 1989. The association of folds and veins in shear zones. *J. Struct. Geol.* **11**, 949–957.

Lister, G. S. & Williams, P. F. 1979. Fabric development in shear zones: theoretical controls and observed phenomena. *J. Struct. Geol.* **1**, 283–297.

Lister, G. S. & Williams, P. F. 1983. The partitioning of deformation in flowing rock masses. *Tectonophysics* **92**, 1–33.

Mattauer, M. 1975. Sur le mecanisme de formation de la schistosite dans l'Himalaya. *Earth & Planet. Sci. Lett.* **28**, 144–154.

Mattauer, M. 1986. Intracontinental subduction, crust-mantle decollement and crustal stacking wedge in the Himalaya and other collision belts. In: *Collision Tectonics* (edited by Coward, M. P. & Ries, A. C.). *Spec. Publs geol. Soc. Lond.* **19**, 363–381.

Means, W. D., Hobbs, B. E., Lister, G. S. & Williams, P. F. 1980. Vorticity and non-coaxiality in progressive deformations. *J. Struct. Geol.* **2**, 371–378.

Mitra, S. 1976. A quantitative study of deformation mechanisms and finite strain in quartzites. *Contr. Miner. Petrol.* **59**, 203–226.

Mitra, S. 1978. Microscopic deformation mechanisms and flow laws in quartzites within the South Mountain anticline. *J. Geol.* **86**, 129–135.

Ottino, J. M. 1989. *The Kinematics of Mixing: Stretching, Chaos and Transport*. Cambridge University Press, New York.
Passchier, C. W. 1986. Flow in natural shear zones—the consequences of spinning flow regimes. *Earth Planet. Sci. Lett.* **77**, 70–80.
Passchier, C. W. 1990. Reconstruction of deformation and flow parameters from deformed vein sets. *Tectonophysics* **180**, 185–199.
Platt, J. P. 1983. Progressive refolding in ductile shear zones. *J. Struct. Geol.* **5**, 619–622.
Platt, J. P. & Behrmann, J. H. 1986. Structures and fabrics in a crustal-scale shear zone, Betic Cordillera, SE Spain. *J. Struct. Geol.* **8**, 15–33.
Ramberg, H. 1975. Particle paths, displacement and progressive strain applicable to rocks. *Tectonophysics* **28**, 1–37.
Ramsay, J. G. 1980. Shear zone geometry: a review. *J. Struct. Geol.* **2**, 83–89.
Ramsay, J. G. & Graham, R. H. 1970. Strain variation in shear belts. *Can. J. Earth Sci.* **7**, 786–813.
Ramsay, J. G. & Huber, I. 1983. *The Techniques of Modern Structural Geology, Volume* 1: *Strain Analysis*. Academic Press, London.
Sengupta, S. 1983. Folding of boudinaged layers. *J. Struct. Geol.* **5**, 197–210.
Sibson, R. H. 1977. Fault rocks and fault mechanisms. *J. geol. soc. Lond.* **133**, 191–213.
Truesdell, C. A. 1954. *The Kinematics Of Vorticity*. Indiana University Press, Bloomington, Indiana.
Truesdell, C. A. 1965. *The Elements of Continuum Mechanics*. Springer, New York.
Von Burns, V. & Talbot, C. J. 1986. Formation of subglacial intrusive clastic sheets in the Dwyka formation of northern Natal, South Africa. *J. sedim. Petrol.* **56**, 35–44.
Williams, P. F. 1977. Foliation: a review and discussion. *Tectonophysics* **39**, 305–328.
Williams, P. F. & Schoneveld, C. 1981. Garnet rotation and the development of axial crenulation cleavage. *Tectonophysics* **78**, 307–334.

APPENDIX A
DERIVATION OF EQUATION (12)

Differentiating (11) gives:

$$\frac{dW_b}{dt} = \frac{1}{S}\left(\frac{d}{dt}\oint_C \mathbf{v}\,d\mathbf{x} - \frac{\partial \ln S}{\partial t}\oint_C \mathbf{v}d\mathbf{x}\right), \tag{A1}$$

where the material boundary **C** and the area of the deformation S are both functions of time.

According to Ottino (1989, equation 2.10.1, p. 37):

$$\frac{d}{dt}\oint_C \mathbf{v}\,d\mathbf{x} = \oint_C \frac{D\mathbf{v}}{Dt}d\mathbf{x} + \oint_C \mathbf{v}\mathbf{L}\,d\mathbf{x} \tag{A2}$$

since:

$$\oint_C \mathbf{v}\mathbf{L}\,d\mathbf{x} = \oint_C \mathbf{v}\,d\mathbf{v} \equiv 0 \tag{A3}$$

therefore:

$$\frac{dW_b}{dt} = \frac{1}{S}\oint_C \left(\frac{D\mathbf{v}}{Dt} - \frac{\partial \ln S}{\partial t}\mathbf{v}\right)d\mathbf{x}. \tag{A4}$$

If $D\mathbf{v}/Dt = 0$ along **C**, (A4) becomes:

$$\frac{dW_b}{dt} = -\frac{\partial \ln S}{\partial t}\frac{1}{S}\oint_C \mathbf{v}\,d\mathbf{x}. \tag{A5}$$

Incorporating (11), we have:

$$\frac{dW_b}{dt} = -\frac{\partial \ln S}{\partial t}W_b. \tag{A6}$$

Solving (A6) gives:

$$W_b S = \text{constant}. \tag{A7}$$

APPENDIX B
DERIVATION OF THE DEFORMATION GRADIENT TENSOR F

The establishment of the reference frame for the derivation of the deformation gradient tensor is described in the text (Figs. 6a & b).

(I) *The reference configuration is when the initial angle is* 0 (0-*configuration*)

$$AD = MN = A_0D_0 \sec\phi = b\sec\phi$$
$$b^2 = 2AM \cdot MN$$
$$AM = \tfrac{1}{2}b\cos\phi$$
$$OA^2 = AM^2 + OM^2 - 2AM \cdot OM\cos\phi$$
$$= a^2 + (ab + \tfrac{1}{4}b^2)\sin^2\phi$$
$$OK^2/(x_1^0)^2 = OA^2/a^2 = 1 + (b/a + \tfrac{1}{4}b^2/a^2)\sin^2\phi$$

since the local heterogeneity factor $R = b^2/(2ab) = \frac{1}{2}b/a$ therefore:

$$OK^2/(x_1^0)^2 = 1 + R(2+R)\sin^2\phi$$
$$OL^2/(x_2^0)^2 = KP^2/(x_2^0)^2 = \sec^2\phi$$

therefore:

$$x_1 = OK\cos\beta + KP\sin\phi$$
$$= [1 + R(2+R)\sin^2\phi]^{1/2}\cos\beta x_1^0 + tan\,\phi x_2^0$$
$$x_2 = OK\sin\beta + KP\cos\phi$$
$$= [1 + R(2+R)\sin^2\phi]^{1/2}\sin\beta x_1^0 + x_2^0$$

where $\tan\beta = R\sin\phi\cos\phi/(1 + R\sin^2\phi)$; $\tan\phi = \gamma$ therefore the deformation gradient tensor $\mathbf{F}(t)$ is:

$$\mathbf{F}(t) = \begin{bmatrix} \mathbf{A}\cos\beta & \tan\varphi \\ \mathbf{A}\sin\beta & 1 \end{bmatrix},$$

where $\mathbf{A} = [1 + R(2+R)\sin^2\phi]^{1/2}$.

(II) *The reference configuration is when the initial angle is* ϕ_0 (ϕ_0-configuration)

The transformation from ϕ_0-configuration (x_1^0, x_2^0) to 0-configuration (x_1', x_2') is:

$$\begin{bmatrix} x_1' \\ x_2' \end{bmatrix} = \begin{bmatrix} 1 & -\tan\varphi_0 \\ \mathbf{A}_0\sin\beta_0 & \mathbf{A}_0\cos\beta_0 \end{bmatrix}\begin{bmatrix} x_1^0 \\ x_2^0 \end{bmatrix},$$

where $\mathbf{A}_0 = [1 + R(2+R)\sin^2\phi]^{1/2}$; $\tan\beta_0 = R\sin\phi_0\cos\phi_0/(1 + R\sin^2\phi_0)$.

The transformation from 0-configuration to ϕ-configuration is:

$$\begin{bmatrix} x_1 \\ x_2 \end{bmatrix} = \begin{bmatrix} \mathbf{A}\cos\beta & \tan\varphi \\ \mathbf{A}\sin\beta & 1 \end{bmatrix}\begin{bmatrix} x_1' \\ x_2' \end{bmatrix}.$$

Therefore the transformation from ϕ_0-configuration to ϕ-configuration is:

$$\begin{bmatrix} x_1 \\ x_2 \end{bmatrix} = \begin{bmatrix} \mathbf{A}\cos\beta & \tan\varphi \\ \mathbf{A}\sin\beta & 1 \end{bmatrix}\begin{bmatrix} 1 & -\tan\varphi_{\varphi_0} \\ -\mathbf{A}_0\sin\beta_0 & \mathbf{A}_0\cos\beta_0 \end{bmatrix}\begin{bmatrix} x_1^0 \\ x_2^0 \end{bmatrix}$$

thus the deformation gradient tensor $\mathbf{F}(t)$ is:

$$\mathbf{F}_{\varphi_0}(t) = \begin{bmatrix} \mathbf{A}\cos\beta & \tan\varphi \\ \mathbf{A}\sin\beta & 1 \end{bmatrix}\begin{bmatrix} 1 & -\tan\varphi_0 \\ -\mathbf{A}_0\sin\beta_0 & \mathbf{A}_0\cos\beta_0 \end{bmatrix}.$$